

# Radiative forcing by anthropogenic surface albedo change before and since 1750

Hadley Centre technical note 70

*Richard A. Betts, Kees Klein Goldewijk, Navin Ramankutty*

August 2006



# Radiative forcing by anthropogenic surface albedo change before and since 1750

Richard A. Betts\*, Kees Klein Goldewijk<sup>#</sup> and Navin Ramankutty<sup>†</sup>

\* Met Office, Hadley Centre for Climate Change, Exeter, UK.

[richard.betts@metoffice.gov.uk](mailto:richard.betts@metoffice.gov.uk)

<sup>#</sup> Netherlands Environmental Assessment Agency (MNP), Bilthoven, The Netherlands

<sup>†</sup>Department of Geography, McGill University, Montreal, Canada

## Abstract

A radiative transfer model was used within a GCM to simulate the global shortwave radiation budget with natural vegetation cover and with the vegetation estimated for 1750, 1850, 1900, 1950 and 1990. Relative to the natural vegetation state, the global mean shortwave radiative forcing due to land cover change by 1750 was simulated as  $-0.06 \text{ Wm}^{-2}$ . The local forcing reached  $-2 \text{ Wm}^{-2}$  over Europe, China and India, indicating a significant cooling influence on climate through agricultural activity before fossil fuel burning began. The description of the pre-industrial climate as “pre-anthropogenic” is therefore inappropriate. The global forcing simulated at 1990 relative to 1750 was  $-0.18 \text{ Wm}^{-2}$ , of comparable magnitude with estimated forcings due to aerosols, ozone, and solar variability. Climate model simulations intended for the detection and attribution of climate change should therefore include changes in surface albedo.

## Introduction

Forty-nine million ha of the global land surface is currently classified as either crops, pasture or grazing, meaning that at least 34% of the global land surface is subject to direct alteration by human activities. The albedo of agricultural land can be very different to that of a natural landscape, especially if the latter was forest, with the albedo of open land being generally higher than forested land. Changes in surface albedo change induce a forcing of climate by perturbing the shortwave radiation budget (Sagan *et al*, 1979). The effect is particularly accentuated when snow is present (Betts, 2000), and surface albedo change may therefore provide the dominant influence of mid- and high-latitude land cover change on climate (Bonan *et al*, 1992; Betts 2001; Bounoua *et al*, 2002).

The present-day global mean radiative forcing due to land cover change relative to the natural state has been variously estimated as  $-0.4 \text{ Wm}^{-2}$  (Hansen *et al*, 1997),  $-0.2 \text{ Wm}^{-2}$  (Betts, 2001) and  $-0.08 \text{ Wm}^{-2}$  (Govindasamy *et al*, 2001). These estimates are similar to those for other forcing agents such as ozone, aerosols, solar variability and most greenhouse gases except  $\text{CO}_2$  and  $\text{CH}_4$ .

The pre-industrial era (pre-1750) is widely regarded as being free from anthropogenic influence on climate. However, since large parts of Europe and south-east Asia have already been deforested before the industrial revolution, the resulting change in surface albedo could already have been exerting a radiative forcing of climate by the time fossil fuel burning began. Therefore, it may not be realistic to describe the pre-

industrial era as “pre-anthropogenic”. Here, we estimate the extent of this pre-industrial anthropogenic influence.

Other anthropogenic radiative forcings are mainly associated with industrial activity, through the emission of greenhouse gases and aerosols. Comparison of the land use forcing with these forcings (eg: Ramaswamy *et al* 2001) therefore requires an estimate of the forcing relative to the start of industrial era (circa 1750). Since agriculture was already widespread in parts of Europe and Asia by this time, the present-day forcing relative to 1750 is likely to be different to the forcing relative to naturally-vegetated state. Estimates of this presented in the IPCC Third Assessment Report (Ramaswamy *et al* 2001) simply assumed that 50% of the current agricultural area was present by 1750, and hence that the forcing relative to 1750 was 50% of that estimated relative to natural. However, historical reconstructions suggest that only approximately 10 million ha were under some sort of agricultural practice by 1750, which is 22 % of the current agricultural area (Klein Goldewijk, 2001). Moreover, the magnitude of forcing by a given form of vegetation change depends strongly on local conditions, specifically snow cover, so a proper estimate of forcing relative to 1750 will require consideration of where land cover changes took place.

Here we use reconstructions of past land cover to perform a spatially-explicit simulations of radiative forcing at 1750, 1850, 1900, 1950 and 1990 relative to natural (hereafter “NAT”). These show how magnitude and pattern of radiative forcing prior to fossil fuel burning, how these have changed over the last 250 years, and allow diagnosis of radiative forcing at 1990 relative to 1750.

## **The climate model**

The shortwave radiation budget was simulated on a global grid of resolution  $2.5^{\circ} \times 3.75^{\circ}$  using the Edwards-Slingo (1996) radiative transfer scheme within the HadAM3 General Circulation Model (Pope *et al*, 1999). HadAM3 includes the MOSES land surface scheme (Cox *et al* 1999), which parametrizes surface albedo using vegetation-dependent parameters and snow depth (Hansen 1983, Betts 2000). In each gridbox, the parameters representing “snow-free albedo” and “maximum deep-snow albedo” are assigned values dependent on the local vegetation type. Albedo then varies with snow depth within these limits.

## **Representing present and past land cover**

In the standard configuration of HadAM3, the global datasets of the vegetation parameter values are derived using the Wilson and Henderson-Sellers (1985) present-day land cover dataset (hereafter “WHS”). WHS specifies 53 land cover classes, including 11 crop classes and 7 pasture/grazing classes. WHS allows up to 2 classes per  $1^{\circ}$  grid square; a primary class covering 75% of the square, and a secondary class covering 25%. HadAM3 surface parameters are derived at  $1^{\circ}$  resolution from this dataset, then bi-linearly interpolated to the GCM resolution.

WHS captures the broad global patterns of intense agriculture during the 1980s, but more recent studies (Ramankutty and Foley 1999, Klein Goldewijk 2001) provide more precise information on the position and extent of agricultural land use in 1990. However, WHS gives more specific information on individual crop types and also



distinguishes pasture from rough grazing. To use key information from all these sources but also keep land surface parameter fields close to those in the standard well-validated HadAM3, we modified WHS using the more recent datasets. We adjusted the fractions of each WHS class in each  $1^\circ$  gridbox so that the total coverage of crops in each gridbox equalled the crop fraction specified by Ramankutty and Foley (1999) on interpolation to that resolution. Crop types were kept as in WHS, and if Ramankutty and Foley (1999) specified crop where WHS did not, the crop type was assumed to be arable. Pasture and grazing land were unchanged except where necessary to accommodate crop cover changes, as the coverage and precision in WHS is close to that specified by Klein Goldewijk (2001).

To represent past land cover in 1750, 1850, 1900 and 1950, we used a similar technique of modifying the WHS fractions to give agreement with the historical reconstructions of Ramankutty and Foley (1999) and Klein Goldewijk (2001). Crop fractions were adjusted to be consistent with those determined by Ramankutty and Foley (1999) – in most cases this involved a reduction of the present-day fraction, although in some locations such as New England the coverage at some times in the past was greater than at present. Crop types were assumed to be identical to the present-day.

Pasture coverage was adjusted with reference to the  $0.5^\circ \times 0.5^\circ$  Boolean dataset of Klein Goldewijk – where Klein Goldewijk specified no pasture or grazing, any pasture class was removed from WHS. Although Klein Goldewijk (2001) also provide crop cover reconstructions, these were not used here since Ramankutty and Foley (1999) give greater precision through the use of fractions rather than a Boolean approach. While the two crop reconstructions generally agree on the global patterns of crop cover resolvable at  $0.5^\circ$  resolution, there are some differences that are not related to precision. The possible implications of this uncertainty will be discussed later. The global patterns of fraction of land identified as agricultural (either croplands or pasture) at 1750 and 1990 are shown in Figure 1.

Following adjustment of the crop and pasture fractions to the historical state, the fractions of other land cover classes were adjusted so that all fractions summed to 1. Where crops or pasture had reduced, this implied an assumption that the non-agricultural vegetation classes represented the potential natural vegetation of the gridbox. In gridboxes where WHS specified complete coverage of crops and/or pasture, the potential natural vegetation class was inferred from a vegetation model (Woodward *et al.*, 1995), following Betts (2001).

A final dataset represented global vegetation prior to disturbance by agriculture. All crop and pasture classes were simply removed from WHS, and replaced with the appropriate potential natural vegetation class as above. The resulting vegetation distribution (see Betts 2001) agreed well with other estimates (eg: Haxeltine and Prentice, 1996).

Having derived  $1^\circ$  land cover maps of the appropriate form, we derived fields of snow-free and deep-snow albedo parameters and interpolated these to the GCM resolution as usual.

## Experimental Design

We performed a 25-year simulation with HadAM3, setting atmospheric CO<sub>2</sub> to its present-day concentration and prescribing sea-surface temperatures and sea ice to a present-day climatology. On each 6-hourly radiation timestep, surface albedo and the shortwave radiation fluxes were calculated 6 times at each gridbox, one calculation for each historical land cover state. Only the calculations performed with 1990 albedo were passed to the rest of the model, and other the other vegetation parameters set to the 1990 state. The simulated near-surface climate was therefore that of the present-day, retaining consistency with the prescribed sea-surface temperature climatology and atmospheric CO<sub>2</sub> concentration.

For each land surface state, we calculated the surface albedo in each gridbox and the associated outgoing shortwave radiation flux (OSR) at the tropopause. The same global distribution of cloud and snow cover was used in all sets of calculations, so the only difference was surface albedo which depended on the snow-free and deep-snow albedo parameters. The difference in OSR for 2 different land surface states gives the radiative forcing due to surface albedo change (Betts, 2001). Therefore, OSR(1990) – OSR(1750) gives the radiative forcing due to land cover change between 1750 and 1990.

## Results

The difference between the outgoing shortwave fluxes simulated with 1750 albedo and with “natural vegetation” albedo gave the simulated radiative forcing due to deforestation-induced albedo change up until 1750 (Figure 2a). The forcing was approximately  $-2 \text{ Wm}^{-2}$  over Europe and northern China. Although a large proportion of China was cultivated at that time, much of this was in warmer regions where the relative infrequency of snow cover reduced the impact of deforestation on surface albedo. The greatest forcing within China was in Manchuria, where long-lasting snow cover allowed land cover change to exert large impacts on surface albedo.

A forcing of  $-1$  to  $-2 \text{ Wm}^{-2}$  was simulated in central and northern India, but in contrast, the forcing in north-east India and Bangladesh was *positive*  $1 \text{ Wm}^{-2}$ . This resulted from the assumption that the local 1750 croplands were largely rice paddies, as is the case today. The open water results in a low surface albedo. Natural vegetation at these points was allocated the albedo of grassland – although rice paddies are generally in naturally-wet areas, the uncultivated state would probably feature less standing water since this is actively maintained for rice paddies.

Negative radiative forcings were simulated in of some parts of the Americas, but these areas were small since European settlers had arrived only relatively recently and major agricultural expansion had yet to take place. The global mean radiative forcing at 1750 was  $-0.06 \text{ Wm}^{-2}$  (Figure 4, Table 1).

In 1850, the simulated forcing relative to the natural state showed generally similar global patterns to that in 1750 but with increased magnitudes of local forcings (Figure 2b). In most of Eastern Europe the forcing was over  $-3 \text{ Wm}^{-2}$ , and over  $-4 \text{ Wm}^{-2}$  in some locations. Similar increases in forcing were seen in southern China, but in

Manchuria the local forcing had reached approximately  $-4$  to  $-5 \text{ Wm}^{-2}$ . Over the north-east USA, a forcing of  $-1$  to  $-2 \text{ Wm}^{-2}$  was simulated over a wider area than in 1750, reflecting the westward expansion of European settlement. The global mean forcing in 1850 relative to NAT was  $-0.10 \text{ Wm}^{-2}$  (Figure 4, Table 1).

By 1900 North American agriculture had undergone major expansion, and at the GCM resolution the land cover was subject to some degree of modification in almost all gridboxes in the eastern half of the present-day conterminous USA. A radiative forcing of  $-1 \text{ Wm}^{-2}$  or more is simulated over that region, with the forcing exceeding  $-5 \text{ Wm}^{-2}$  in the intensively cultivated north (Figure 2c). In Europe, India and China the forcing continued to increase in intensity while the extent of the disturbed areas remained similar to that in 1850. The global mean forcing had now more than doubled since 1750, being  $-0.14 \text{ Wm}^{-2}$  by 1900 (Figure 4, Table 1).

Between 1900 and 1950 the forcing intensified by a similar degree in most areas, with local forcings of over  $-5 \text{ Wm}^{-2}$  being simulated in all the main centres of global agriculture (Figure 2d). North American agriculture continued to expand westwards, widening the area of negative radiative forcing. In contrast, however, local forcing decreased in the north-east USA, where cropland abandonment and forest regrowth had led to decreased surface albedo since 1900. The global mean forcing by 1950 was  $-0.18 \text{ Wm}^{-2}$ , three times that of 1750 (Figure 4, Table 1).

The pattern of forcing remained similar up to the final simulation at 1990, with continental-scale expansion being slower than before 1950 but local forcings intensifying due to continued expansion at the sub-grid scale (Figure 2e). The global mean radiative forcing at 1990 relative to NAT was simulated as  $-0.24 \text{ Wm}^{-2}$  (Figure 4, Table 1), slightly more than that previously simulated by Betts (2001) but still less than that by Hansen et al (1997).

The difference between the 1990 and 1750 OSR gives the forcing by surface albedo change since the industrial revolution (Figure 3). The global mean forcing at 1990 relative to 1750 is  $-0.18 \text{ Wm}^{-2}$ , three-quarters of the forcing simulated relative to NAT.

## Discussion and conclusions

This simulation suggests that surface albedo change was exerting a significant radiative forcing by 1750, indicating that humans were already affecting climate through land cover change before the burning of fossil fuels began. The climatic impact of carbon emissions from land clearance would have been small, because the low emission rate could have been largely offset by absorption in the oceans or unconverted land ecosystems. However, unless the land is subsequently abandoned, deforestation leads to a permanent change in surface albedo. Hence a single deforestation event can exert a very long-term radiative forcing relative to the previously undisturbed state.

Deforestation would therefore have exerted a cooling influence in addition to that from solar forcing. The global mean surface albedo forcing in 1750 has been estimated here to be  $0.06 \text{ Wm}^{-2}$ , which is approximately 10% of the global solar

forcing at that time (Crowley 2000) at the Maunder Minimum relative to present-day. However, the local surface albedo forcing over Europe has here been estimated as  $-2.0 \text{ W m}^{-2}$ , so locally the land use forcing may have been 3 to 4 times larger than the solar forcing. Land use change could therefore have contributed to the Northern Hemisphere cold period of the 17<sup>th</sup> Century (the “Little Ice Age”). (Sagan *et al*, 1979; Brovkin *et al*, 1999; Govindasamy *et al*, 2001)

The forcing of  $-0.24 \text{ W m}^{-2}$  simulated for 1990 relative to natural vegetation is slightly more than that previously simulated by Betts (2001) using the WHS dataset alone. This is due to more land being designated as agricultural in this study, mainly because the crop fraction data allows the inclusion of sparse agriculture which may nevertheless be important if present over a wide area. This new estimate still falls between those of  $-0.4 \text{ W m}^{-2}$  (Hansen *et al* 1997) and  $-0.08 \text{ W m}^{-2}$  (Govindasamy *et al* 2001). The simulation by Hansen *et al* (1997) included significant land cover changes in the African savannas, which are not seen in the datasets used here. This may simply reflect differences in the definition of anthropogenic land cover change.

The above results provide the first explicit simulation of the forcing due to land use relative to 1750, a quantity which is important for studies of climate change in the industrial era. By differencing the fluxes at 1990 and 1750, we simulate this forcing to be  $-0.18 \text{ W m}^{-2}$  in the global mean. This is close to that estimated by Hansen *et al* (1997) who simply assumed 50% of current land cover change by 1750 – however, our estimate is based on a more rigorous treatment of land cover change. Our results therefore support the IPCC estimate of  $-0.2 \text{ W m}^{-2}$ , but perhaps suggest that the lower limit of the uncertainty range should be higher than zero.

The pattern of forcing at 1990 relative to 1750 (Figure 3) was similar to that relative to natural vegetation (Figure 1e), the regional-scale forcings being smaller in magnitude by approximately 20%. This is important information because it means that estimates of the pattern of forcing relative to 1750 can be obtained to a reasonably approximation from estimates of the forcing relative to potential natural vegetation, by scaling the forcing linearly in proportion to the global mean forcing.

The global mean surface albedo forcing of  $-0.18 \text{ W m}^{-2}$  over the industrial period is smaller than the global forcing by greenhouse gases ( $2.5 \text{ W m}^{-2}$ , Ramaswamy *et al* 2001); whereas the greenhouse forcing is relatively uniformly distributed across the globe, the albedo changes simulated here were very localised. Nevertheless, the global surface albedo forcing is of a similar magnitude to the forcings by the direct effect of sulphate aerosols, stratospheric and tropospheric ozone, the halocarbons, and  $\text{N}_2\text{O}$  (Ramaswamy *et al*, 2001).

The magnitude of the global mean radiative forcing due to surface albedo change over the last 250 years (Figure 4a) is comparable with other sources of anthropogenic shortwave radiative forcings, namely aerosols (Figure 4b). This is important because changes in the underlying surface albedo could affect the radiative forcing due to aerosols, and conversely, the aerosol loading may modify the forcing due to surface albedo change. Sulphate aerosol loading has changed in much the same regions that have experienced major land surface albedo change (ie: the most populated parts of the temperate regions), although biomass burning aerosol changes are generally in somewhat different areas (less densely populated forest and savanna regions -

Ramaswamy *et al* 2001). Estimates of the time evolution of aerosol forcings and surface albedo forcings may therefore need to be repeated considering changes in each other.

The local annual mean shortwave radiative forcing due to anthropogenic surface albedo change exceeded  $-5 \text{ W m}^{-2}$  in parts of Europe, North America and the cooler regions of Asia (Figures 6 and 7), which is considerably greater than the forcings relative to pre-industrial times exerted by greenhouse gases ( $2 \text{ W m}^{-2}$ ) and the direct effect of sulphate aerosols ( $-1.5 \text{ W m}^{-2}$ ) over these areas (Ramaswamy *et al* 2001). Consequently, although we have concluded that global mean radiative forcing is useful for comparing the global effects of anthropogenic albedo change and other forcings, we also note that the highly regionalised nature of the anthropogenic surface albedo forcing may render such global comparison less useful when considering the implications of different forcings at local scales.

This work has presented 2 key results relating to radiative forcing due to land-use induced surface albedo change. (i) Radiative forcing at 1750 relative to potential natural vegetation, and (ii) radiative forcing at 1990 relative to 1750. The forcing at 1750 has been shown to be significant, so we therefore consider it inappropriate to describe the pre-industrial climate as “pre-anthropogenic”. The forcing since 1750 is also significant, and comparable with other forcings taken into account in historical climate change simulations. Therefore, studies of climate change detection and attribution should therefore consider anthropogenic changes in surface albedo.



## References

- Betts, R. A., 2000: Offset of the potential carbon sink from boreal forestation by decreases in surface albedo. *Nature* **408**, 187-190
- Betts R. A., 2001: Biogeophysical impacts of land use on present-day climate: near-surface temperature change and radiative forcing. *Atmospheric Science Letters*, doi:1006/asle.2001.0023
- Bonan, G.B., D. Pollard, and S. L. Thompson, 1992: Effects of boreal forest vegetation on global climate. *Nature*, **359**, 716-718.
- Brovkin, V., A. Ganapolski, M. Claussen, C. Kubatzki, and V. Petoukhov, 1999: Modelling climate response to historical land cover change. *Global Ecology and Biogeography*, **8**:509-517
- Bounoua, L., R. DeFries, G. J. Collatz, P. Sellers, and H. Khan, 2002: Effects of land cover conversion on surface climate. *Climatic Change*, **52**, 29-64.
- Cox, P. M., R. A. Betts, C. B. Bunton, R. L. H. Essery, P. R. Rowntree and J. Smith, 1999: The impact of new land surface physics on the GCM simulation of climate and climate sensitivity. *Clim. Dyn.* **15**, 183-203
- Crowley T. 2000: Causes of Climate Change Over the Past 1000 Years. *Science*, **289**, 270-277
- Edwards, J. M. & Slingo, A., 1996: Studies with a flexible new radiation code. I: Choosing a configuration for a large-scale model. *Q. J. R. Meteorol. Soc.* **122**, 689-720
- Govindasamy B, P. B. Duffy, and K. Caldeira, 2001: Land use Changes and Northern Hemisphere Cooling. *Geophy. Res. Lett.* **28** (2), 291-294
- Hansen, J., Russell, G., Rind, D., Stone, P., Lacis, A., Lebedeff, S., Ruedy, R. and Travis, L., 1983: Efficient three-dimensional global models for climate studies: models I and II. *Monthly Weather Review*, **111**: 609-662.
- Hansen, J., M. Sato, A. Lacis, and R. Ruedy, 1997b: The missing climate forcing. *Phil. Trans. Royal Soc. London B* **352**, 231-240.
- Haxeltine, A. and I. C. Prentice, 1996: BIOME3: An equilibrium terrestrial biosphere model based on ecophysiological constraints, resource availability, and competition among plant functional types. *Global Biogeochemical Cycles* **10**(4): 693-709.
- Klein Goldewijk, K., 2001: Estimating global land use change over the past 300 years: The HYDE database, *Global Biogeochemical Cycles* **15**(2): 417-433.

Pope, V.D., Gallani, M.L., Rowntree, P.R. and Stratton, R.A., 1999: The impact of new physical parametrizations in the Hadley Centre climate model - HadAM3. *Climate Dynamics*, **16**, (2/3): 123-146.

Ramankutty, N., and J.A. Foley, 1999: Estimating historical changes in global land cover: croplands from 1700 to 1992. *Global Biogeochemical Cycles* **13**(4), 997-1027.

Ramaswamy, V., O. Boucher, J. Haigh, D. Hauglustaine, J. Haywood, G. Myhre, T. Nakajima, G.Y. Shi, S. Solomon, R. Betts, R. Charlson, C. Chuang, J. S. Daniel, A. Del Genio, R. van Dorland, J. Feichter, J. Fuglestad, P. M. de F. Forster, S. J. Ghan, A. Jones, J. T. Kiehl, D. Koch, C. Land, J. Lean, U. Lohmann, K. Minschwaner, J. E. Penner, D. L. Roberts, H. Rodhe, G. J. Roelofs, L. D. Rotstayn, T. L. Schneider, U. Schumann, S. E. Schwartz, M.D. Schwarzkopf, K. P. Shine, S. Smith, D. S. Stevenson, F. Stordal, I. Tegen, and Y. Zhang, 2001: Radiative forcing of climate change. In *Climate Change 2001: The Scientific Basis. Contribution of Working Group I to the Third Assessment Report of the Intergovernmental Panel on Climate Change*, Cambridge, UK: Cambridge University Press, 350-416.

Sagan, C., O. B. Toon and J. B. Pollack, 1979: Anthropogenic albedo changes and the Earth's climate. *Science*, **206**, 1363-1368

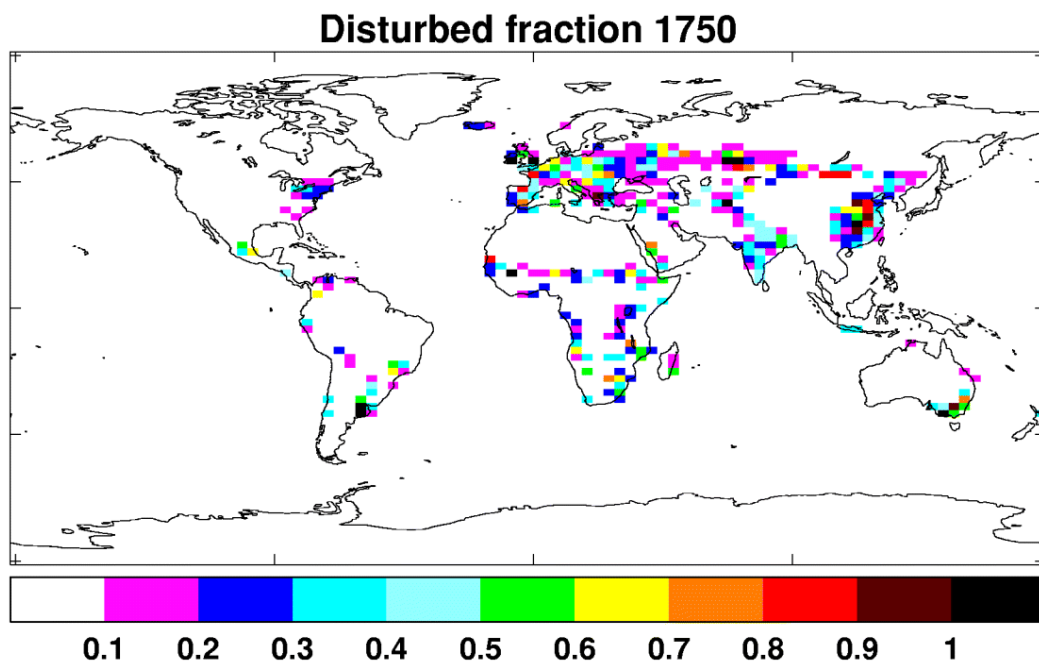
Wilson, M.F. and A.Henderson-Sellers, 1985: A global archive of land cover and soils data for use in general circulation models. *Journal of Climate*, **5**, 119-143

Woodward, FI, TM Smith and WR Emanuel, 1995: A global land primary productivity and phytogeography model. *Global Biogeochemical Cycles*, **9**, 471-490.

**Table 1.** Global areas under agriculture and global mean radiative forcing at 1750, 1850, 1900, 1950 and 1990. Crop areas estimates from Ramakutty and Foley (1999), pasture area estimates from Klein Goldewijk (2001)

Year	Area under crops (million km <sup>2</sup> )	Area under pasture (million km <sup>2</sup> )	Total area under agriculture (million km <sup>2</sup> )	Radiative forcing relative to natural (Wm <sup>-2</sup> )	Forcing relative to 1750 (Wm <sup>-2</sup> )
Natural	0	0			
1750	5.41	6.97	12.38	-0.06	0
1850	8.21	13.10	21.31	-0.10	-0.04
1900	11.44	19.54	30.98	-0.14	-0.08
1950	15.28	29.30	44.58	-0.18	-0.12
1990	17.92	34.50	52.42	-0.24	-0.18

a



b

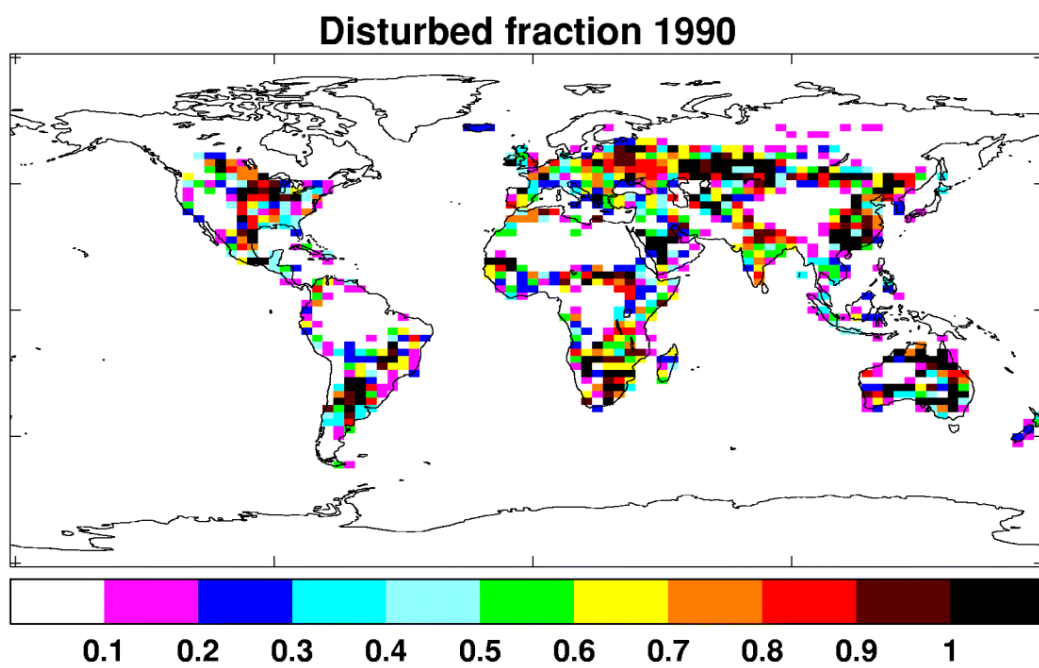
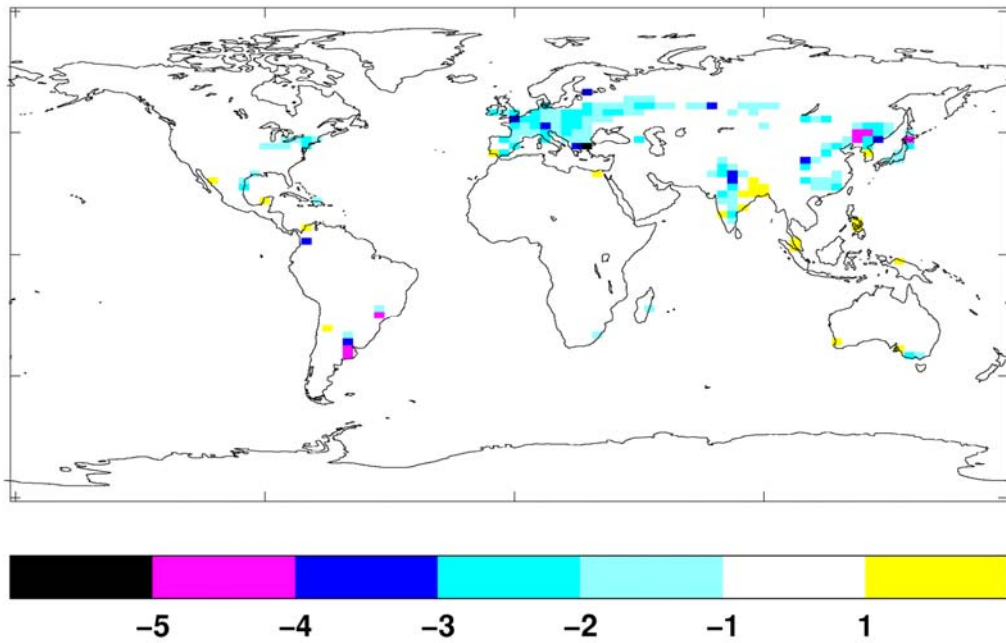


**Figure 1.** Fraction of the land surface at the GCM grid scale defined as under direct human influence (crops plus pasture) in this study, for (a) 1750 and (b) 1990.

**a**



**b**

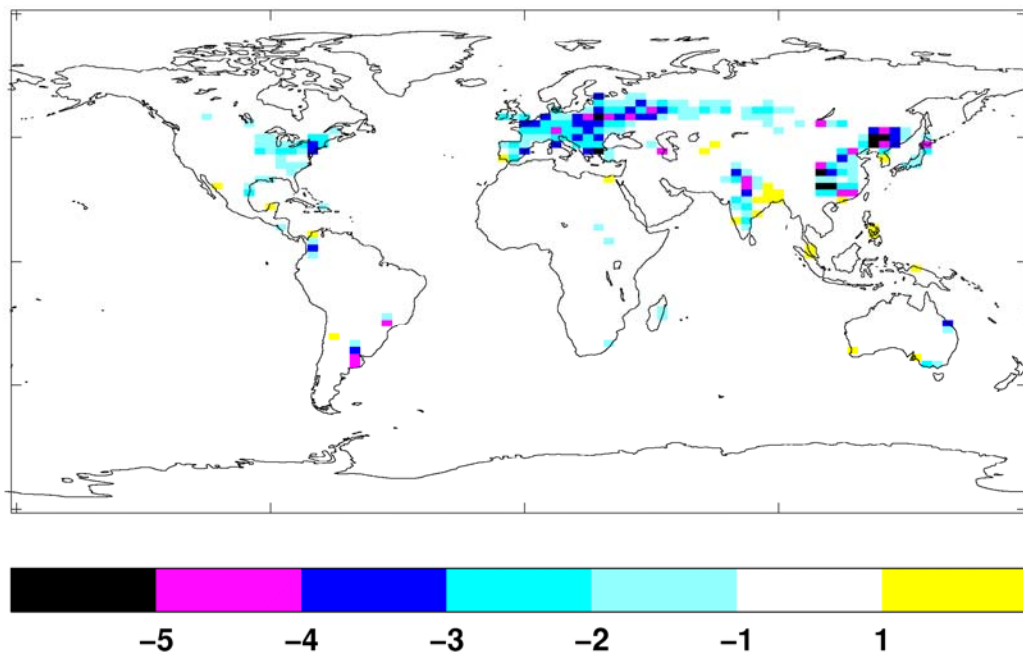
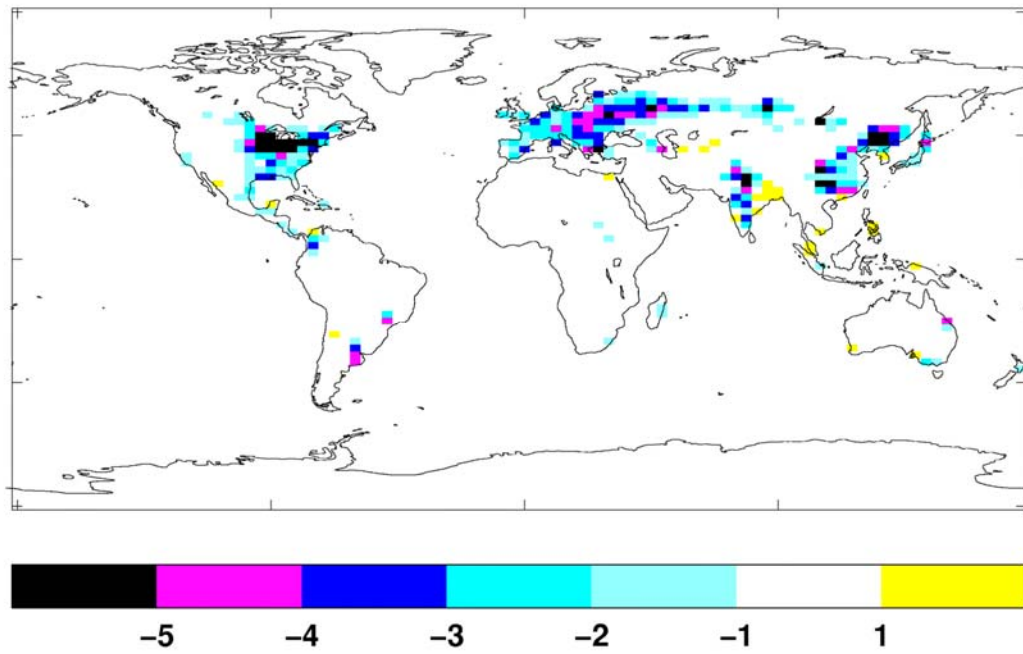


**Figure 2.** Simulated annual mean radiative forcing ( $\text{Wm}^{-2}$ ) at (a) 1750, (b) 1850, (c) 1900, (d) 1950 and (e) 1990 relative to NAT.

c



d

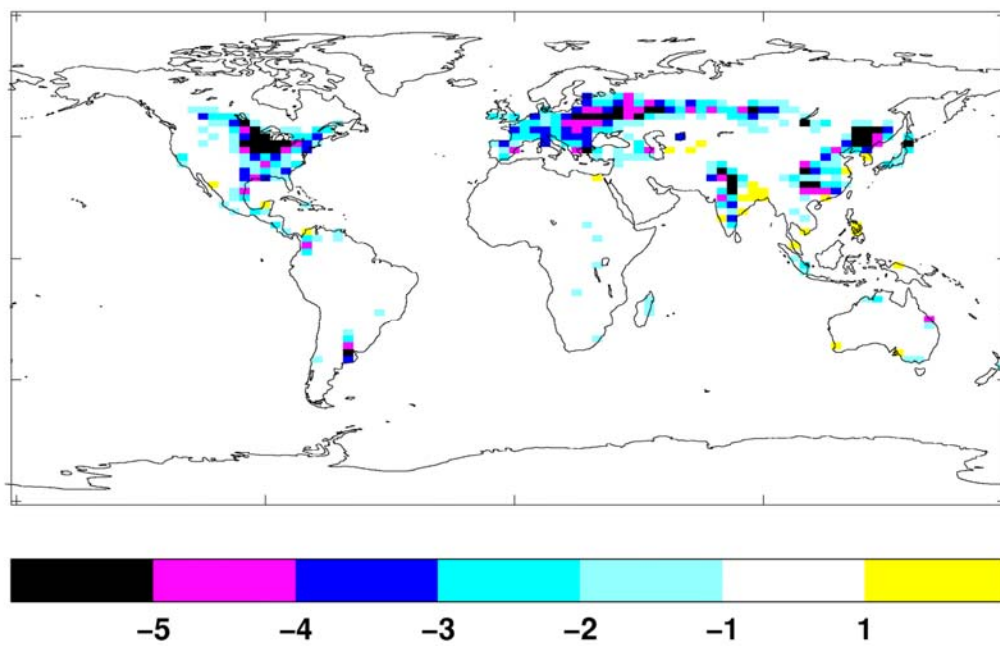


**Figure 2 (continued).** Simulated annual mean radiative forcing ( $\text{Wm}^{-2}$ ) at (a) 1750, (b) 1850, (c) 1900, (d) 1950 and (e) 1990 relative to NAT.



e

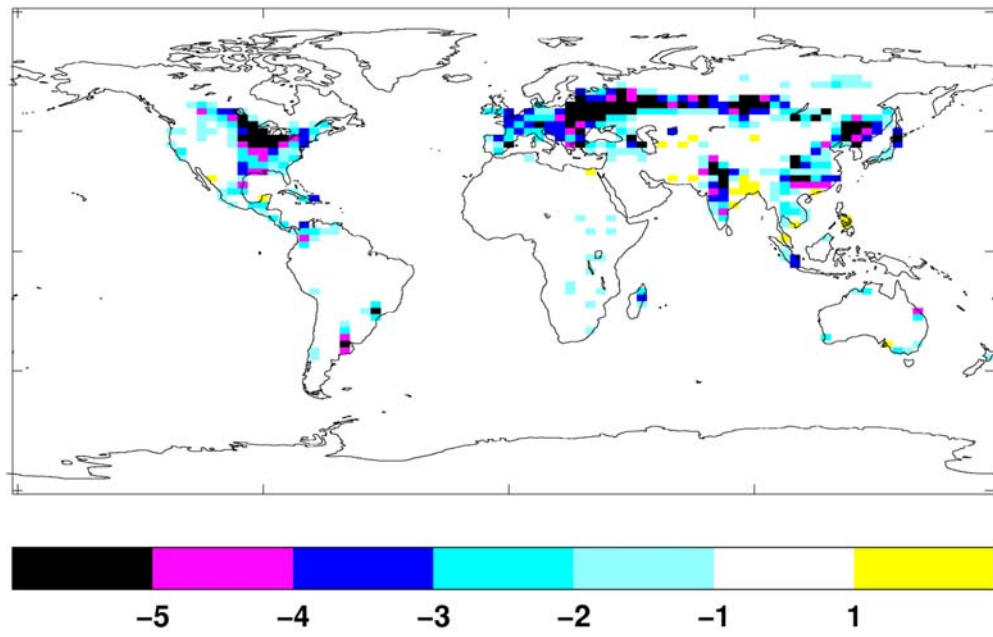


**Figure 2 (continued).** Simulated annual mean radiative forcing ( $\text{Wm}^{-2}$ ) at (a) 1750, (b) 1850, (c) 1900, (d) 1950 and (e) 1990 relative to NAT.

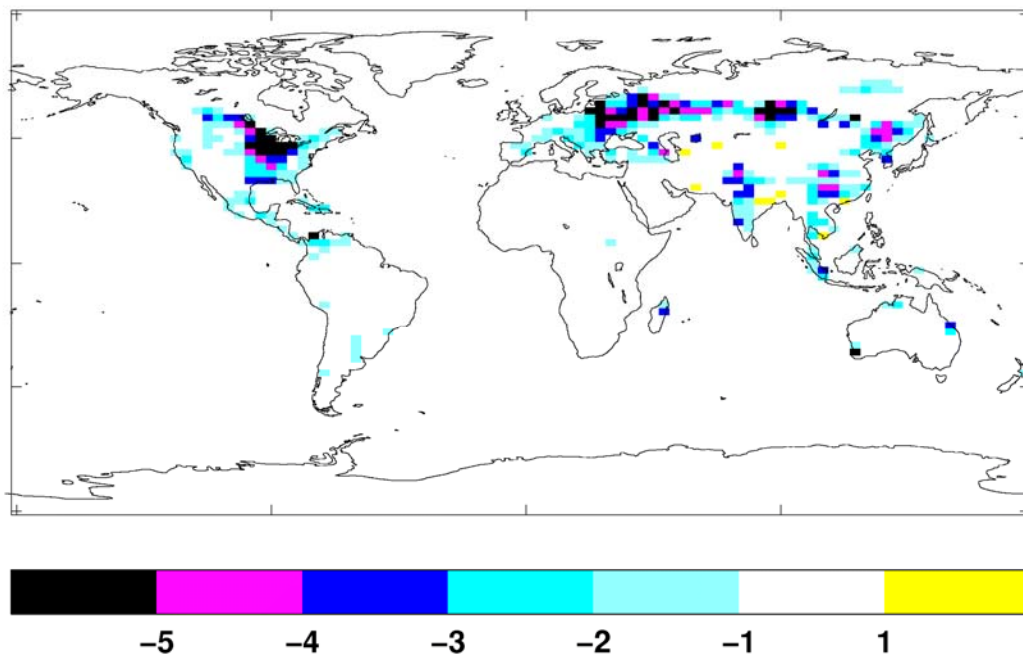
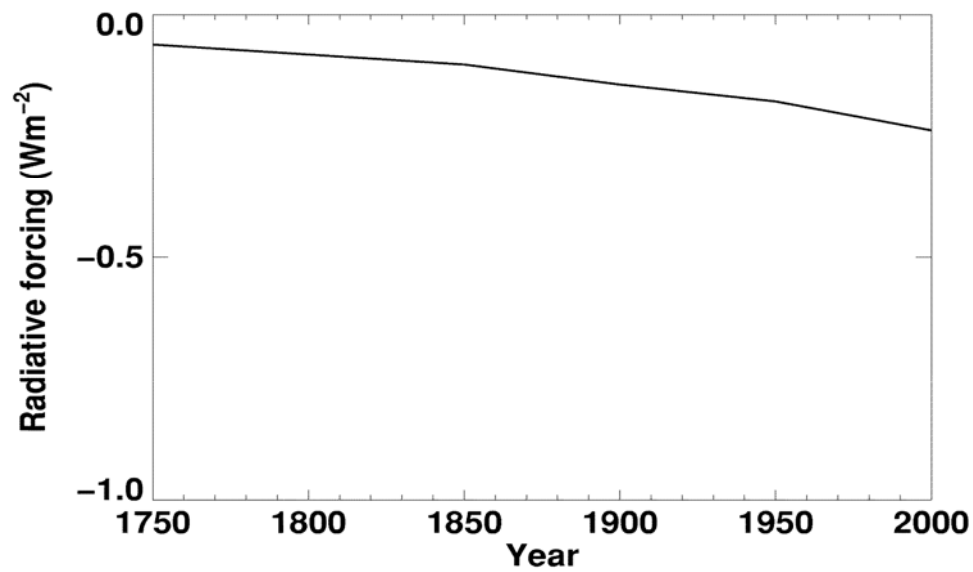


**Figure 3.** Simulated annual mean radiative forcing ( $\text{Wm}^{-2}$ ) in 1990 relative to 1750.

a



b

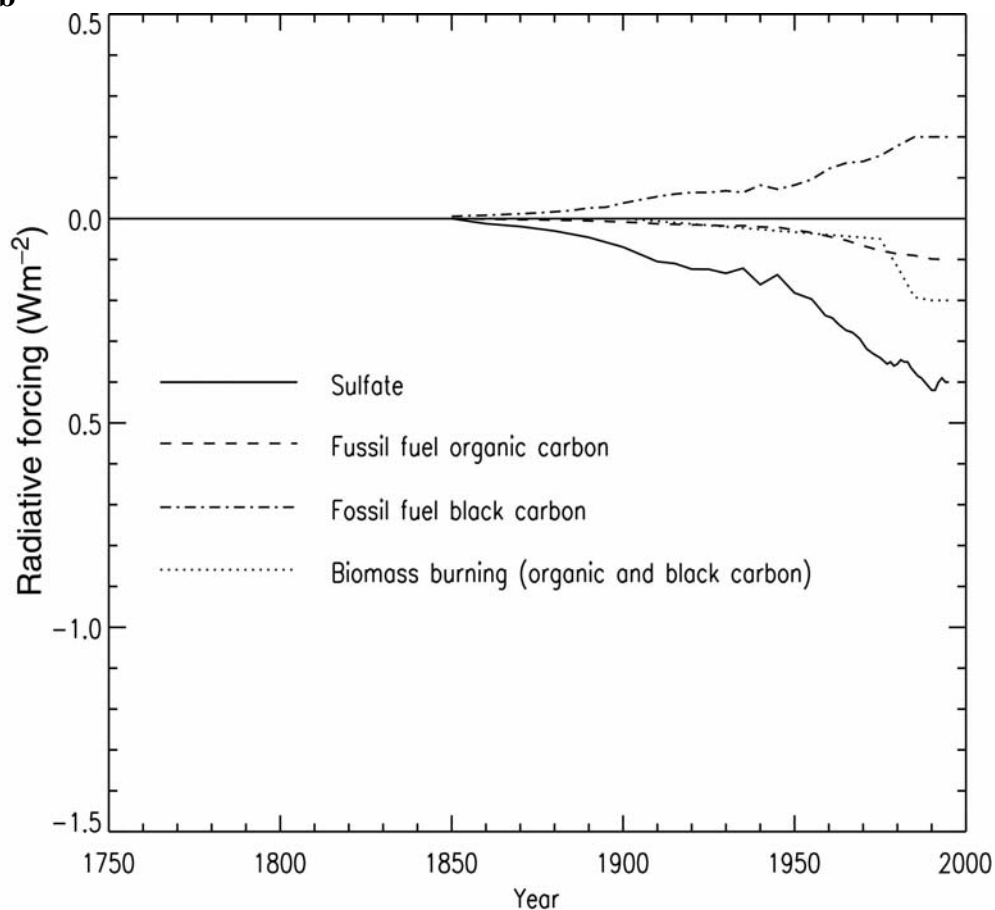


**Figure 4.** (a) Time series of simulated global mean shortwave radiative forcing due to land use change relative to natural vegetation. (b) Time series of simulated global mean radiative forcings due to anthropogenic aerosols (copyright IPCC, reproduced with permission)